Coupling Ca^{2+} store release to Icrac channel activation in B lymphocytes requires the activity of Lyn and Syk kinases

S. Clare Chung,[1] Andre Limnander,[2,3] Tomohiro Kurosaki,[4,5] Arthur Weiss,[2,3] and Juan I. Korenbrot[1]

[1]Department of Physiology, [2]Department of Medicine, and [3]Howard Hughes Medical Institute, School of Medicine, University of California, San Francisco, San Francisco, CA 94143
[4]Department of Molecular Genetics, Institute for Liver Research, Kansai Medical University, and [5]Laboratory for Lymphocyte Differentiation, RIKEN Research Center for Allergy and Immunology, Moriguchi 570-8506, Japan

Activation of the B cell receptor complex in B lymphocytes causes Ca^{2+} release from intracellular stores, which, in turn, activates ion channels known as Icrac. We investigated the mechanisms that link Ca^{2+} store release to channel gating in DT40 B lymphocyte cell lines genetically manipulated to suppress the expression of several tyrosine kinases: Btk, Lyn, Syk, and the Blnk adaptor molecule. The simultaneous but not the independent suppression of Lyn and Syk expression prevents the activation of Icrac without interfering with thapsigargin-sensitive Ca^{2+} store release. Icrac activation by Ca^{2+} is reversed in mutant cells by the homologous expression of the missing kinases. Pharmacological inhibition of kinase activity by LavendustinA and PP2 cause the same functional deficit as the genetic suppression of enzyme expression. Biochemical assays demonstrate that kinase activity is required as a tonic signal: targets must be phosphorylated to link Ca^{2+} store release to Icrac gating. The action of kinases on Icrac activation does not arise from control of the expression level of the stromal interaction molecule 1 and Orai1 proteins.

Introduction

In mature B lymphocytes, binding of antigen or antireceptor antibody to the B cell receptor (BCR) complex causes a sustained rise in intracellular free Ca^{2+}, which, in turn, regulates proliferation and differentiation of the cells into either memory or antibody-secreting ones (for review see Kurosaki, 2000). The increase in cytoplasmic Ca^{2+} arises from two successive events: first, there occurs a transient Ca^{2+} release from intracellular stores initiated by a rise in free inositol 1,4,5-trisphosphate (IP$_3$; for review see Berridge et al., 2003). In turn, the emptying of Ca^{2+} stores activates Icrac (Ca^{2+} release activated) ion channels. The channels are Ca^{2+} permeable, and Ca^{2+} influx via these channels results in a sustained elevation of cytoplasmic free Ca^{2+} (Parekh and Penner, 1997; for review see Lewis, 1999). The molecular identity of the Icrac channels has yet to be fully determined, but recent studies demonstrate that the protein Orai1 (also called CRACM1) is an integral component of the channel and is associated with its Ca^{2+} selectivity filter (Vig et al., 2006a; Yeromin et al., 2006). Orai1, a gene product identified

in severe combined immunodeficiency patients (Feske et al., 2006), was discovered to be important in Icrac function through RNAi screens (Feske et al., 2006; Vig et al., 2006b; Zhang et al., 2005).

Tyrosine kinase activity is absolutely required for activation of the BCR–Ca^{2+} signaling pathway (for review see Kurosaki, 2000). In the absence of kinase function, the sequence of molecular events linking BCR activation to IP$_3$ production fails because the normal phosphorylation and activation of PLCγ, the enzyme that produces IP$_3$, does not occur. The BCR complex is a multimer consisting of membrane Ig associated with Ig α/β heterodimers. The BCR complex interacts with and is phosphorylated by one or more of the following members of the Src kinase family: Lyn, Fyn, and/or Blk. In addition to the Src kinase family, two other tyrosine kinases participate in the BCR–Ca^{2+} signaling pathway: Syk (Syk family) and Btk (Tec family). All three tyrosine kinase families participate in PLCγ activation. Furthermore, tyrosine kinase–dependent activation of PLCγ is facilitated by adaptor or linker proteins such as Blnk (for review see Kurosaki, 2000). Whether these enzymes play a role in the events that link the emptying of Ca^{2+} stores to Icrac activation has not been investigated directly. However, indirect

Correspondence to Juan I. Korenbrot: juan.korenbrot@ucsf.edu

Abbreviations used in this paper: BCR, B cell receptor; IP$_3$, inositol 1,4,5-trisphosphate; STIM1, stromal interaction molecule 1; TG, thapsigargin.
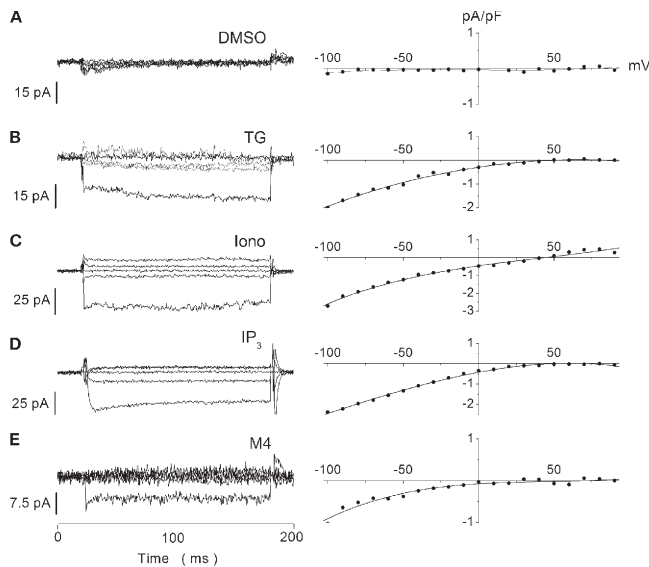
A DMSO

15 pA

pA/pF

-100   -50   50   mV

B TG

15 pA

-100   -50   50

C Iono

25 pA

-100   -50   50

D IP$_3$

25 pA

-100   -50   50

E M4

7.5 pA

-100   -50   50

0   100   200
Time (ms)

Figure 1. **Activation of Icrac in wild-type DT40 cells by different agents.** Voltage-clamped membrane currents measured at room temperature in normal Ringer's solution. Cells were held at 0 mV, and currents were activated by 160-ms duration voltage steps between −100 and 90 mV in 10-mV steps. I-V curves were measured in the steady state of activated Icrac currents between 2 and 10 min after cell stimulation. Currents activated at −100, −30, 0, 30, and 90 mV are shown. (A) Control cell treated with delivery vehicle alone (0.1% DMSO). (B) Treated with 1 µM extracellular TG. (C) Treated with 0.5 µM extracellular ionomycin. (D) Treated with 60 µM IP$_3$ delivered by diffusion from the lumen of the tight-seal electrode. (E) Treated with a 1:400 dilution of extracellular M4, a specific BCR antibody. To the right of each current set is that cell's I-V curve measured after chemical activation. The current is the mean amplitude measured in the 60–160-ms interval after voltage step onset. To compare among cells of varying size, the current amplitude in each cell was normalized by the cell's membrane surface, which was measured as membrane capacitance. Every one of the drugs tested activated the Icrac current, which is defined by its characteristic inward rectifying features.

Table I. **Stationary current amplitude at −100 mV in wild-type DT40 cells stimulated to cause Ca^{2+} store release**

Mode of stimulation	Current amplitude	n
DMSO carrier	0.13 ± 0.15	10
1 µM TG	1.25 ± 0.40	20
0.5 µM ionomycin	1.60 ± 0.35	10
60 µM IP$_3$	1.29 ± 0.28	43
1:400 M4 antibody	1.09 ± 0.20	5

Current amplitude is given as pA/pF ± SEM.

studies using pharmacological blockers of tyrosine kinase function have suggested that the enzymes may play a role in linking Ca^{2+} store release and Ca^{2+} influx (Lee et al., 1993, Sargeant et al., 1993a,b). In this study, we provide direct evidence of a role for kinases in the link between Ca^{2+} store emptying and Icrac activation, and we identify some of the specific enzymes involved.

Two general classes of mechanisms have been proposed to link the store release of Ca^{2+} to Icrac activation. The first class proposes that Icrac channels are structurally linked to the Ca^{2+}-containing stores and that their activation depends on a conformational coupling between the store and the plasma membranes (Irvine, 1990; Petersen and Berridge, 1996; Kiselyov et al., 2001). The second class of mechanisms proposes that second messenger molecules accomplish this link through Ca^{2+}-dependent activation of target proteins. Over time, several plausible messenger proteins have been proposed: G proteins (Bird and Putney, 1993; Fasolato et al., 1993; Jaconi et al., 1993; Petersen and Berridge, 1995), PKC (Parekh and Penner, 1995), tyrosine kinases (Lee et al., 1993; Sargeant et al., 1993a,b; Rosado et al., 2000), Ca^{2+} influx factor (Randriamampita and Tsien, 1993; Csutora et al., 1999), inositol 1,3,4,5-tetrakisphosphate (Luckhoff and Clapham, 1992), and cytochrome P-450 (Alvarez et al., 1992). Recently, however, a compelling case has been

developed that identifies stromal interaction molecule 1 (STIM1) as a messenger protein between Ca^{2+} release and Icrac gating (Liou et al., 2005; Roos et al., 2005; Zhang et al., 2005). Simultaneous overexpression of STIM1 and Orai1 but not either alone facilitates the activation of Icrac (Peinelt et al., 2006). STIM1 is a membrane-bound Ca^{2+}-binding protein (its structure includes an EF hand) located in the ER. STIM1 acts as a Ca^{2+} sensor: store Ca^{2+} depletion causes STIM1 to cluster as discrete aggregates (puncta) that relocalize to ER membrane areas juxtaposed to the plasma membrane. STIM1 puncta co-localize with Orai1, and Ca^{2+} release–activated channels open at or near the sites where this protein nexus forms (Luik et al., 2006; Wu et al., 2006).

To further our understanding of the mechanisms that couple Ca^{2+} store release to Icrac gating, we investigated the features of Icrac and Ca^{2+} store release in a chicken B lymphocytic cell line, DT40, in which the expression of specific kinases can be genetically manipulated (Takata et al., 1994; Takata and Kurosaki, 1996; Ishiai et al., 1999). Our results indicate that Lyn or Syk tyrosine kinases are absolutely required to link the Ca^{2+} released from intracellular stores to Icrac gating: when the simultaneous expression of the enzymes is genetically suppressed, Icrac is not activated by the release of intracellular Ca^{2+} stores. This effect is reversible and specific and can be mimicked by the application of drugs that suppress kinase enzymatic activity in wild-type cells. The kinase effects do not arise from changes in the expression levels of either Orai1 or STIM1. Moreover, the release of Ca^{2+} does not change the level of the phosphorylation of Syk, a measure of its enzymatic activity, and only small changes are detected in Lyn. Therefore, tonic signals that generate small pools of phospho-Lyn and -Syk appear to be required for Icrac activation.

Results

To investigate the role of tyrosine kinases in the molecular mechanisms underlying Icrac activation, we studied the electrophysiological properties of wild-type and genetically modified DT40 cells engineered to suppress the expression of specific proteins of interest.

Features of Icrac in wild-type DT40 cells

We measured voltage-clamped membrane currents at room temperature and tested the response to various agents that cause the release of Ca^{2+} from intracellular stores: (1) thapsigargin (TG) blocks the constitutively active Ca^{2+} transport into ER
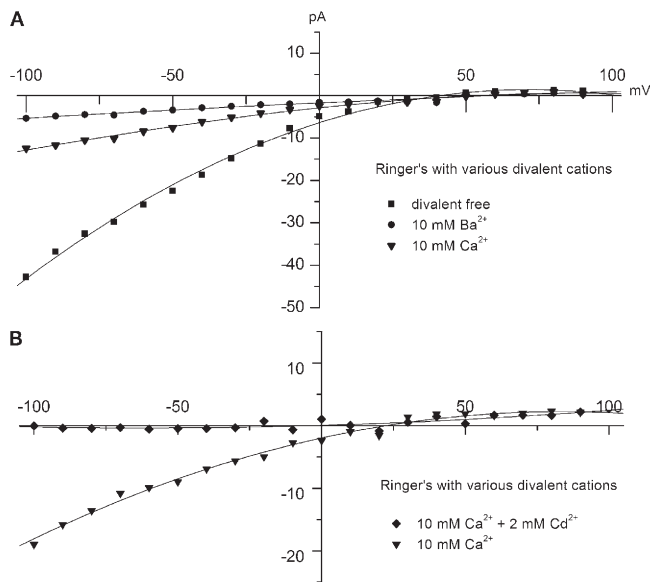
Figure 2. **Ion selectivity of Icrac in DT40 cells treated with 60 μM intracellular IP$_3$.** (A) Steady-state current amplitudes measured in the same cell between −100 and 90 mV in the sequential presence of extracellular Ringer's solution containing 150 mM Na$^+$ and either free of divalent cations (squares; with 2 mM EGTA), with 10 mM Ca^{2+} (triangles), or with 10 mM Ba^{2+} (circles). (B) I-V curve of Icrac in different cells measured in the presence of 150 mM Na$^+$ and either 10 mM Ca^{2+} (triangles) or 10 mM Ca^{2+} with 2 mM of added Cd^{2+} (diamonds).

Figure 3. **Activation of Icrac in DT40 cells by 60 μM intracellular IP$_3$.** Voltage-clamped membrane currents measured at room temperature in cells bathed with normal Ringer's solution. Cells were held at 0 mV. Currents activated at −100, −30, and 0 mV are shown. To the right of each current set is that cell's steady-state I-V curve after activation. (A–D) Blnk- (A), Lyn- (B), Btk- (C), and Syk-deficient (D) cells. (E) Cell deficient in both Lyn and Syk. The characteristic inwardly rectifying Icrac current is completely absent only in cells lacking both Lyn and Syk tyrosine kinases.

stores mediated by the ATP-dependent Ca^{2+} pump (*sarcoplasmic/ER Ca^{2+} ATPase*); (2) M4, a mAb, specifically activates the B cell antigen receptor (BCR), which, in turn, activates PLCγ and elevates cytoplasmic IP$_3$; (3) IP$_3$ delivered via the tight-seal electrode, which causes Ca^{2+} release through interaction with its specific receptor on the ER membrane; and (4) ionomycin, an ionophore that renders membranes permeable to divalent cations. Each of the four reagents slowly activated a stationary inward membrane current at −90 mV (Fig. 1 and Table I). This current was unambiguously identified as Icrac because of its biophysical features (Lewis and Cahalan, 1989; Hoth and Penner, 1992; McDonald et al., 1993; Zweifach and Lewis, 1993).

The characteristics of Icrac that we report were measured at various times, starting 120 s after first adding the stimulant and as long as 10 min thereafter. We did not observe remarkable differences throughout this time. We did not measure in detail the time course of Icrac development in our experiments, but a previous study indicates that IP$_3$ fully activates the current within 150 s (Kiselyov et al., 2001), and TG activates the current 60–120 s after adding the stimulant (see Fig. 6 and the section Effect of TG on cytoplasmic Ca^{2+}…). We identified the current activated by the various stimulants as Icrac because (1) its I-V curve is inwardly rectifying and has a reversal potential between 40 and 50 mV; (2) it activates with a substantial delay relative to the moment of drug delivery; (3) it exhibits an anomalous mole fraction effect between Na$^+$ and Ca^{2+} ions; (4) in the presence of divalent cations, it strongly selects divalent over monovalent cations but does not distinguish among some divalent cations (Ba^{2+} is permeant, although somewhat less than Ca^{2+}); and (5) it is blocked by Cd^{2+}.
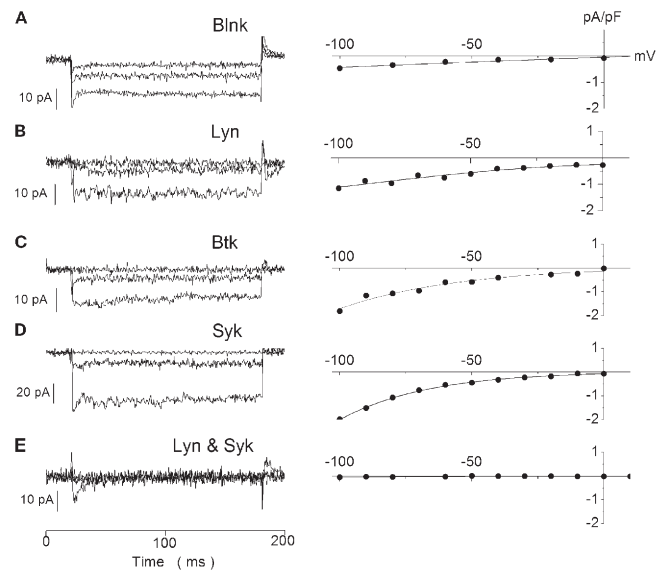
The ion selectivity features of Icrac activated by IP$_3$ are illustrated in Fig. 2. Current was activated by IP$_3$ delivered by diffusion from the lumen of the tight-seal electrode. In the same cell, we first measured the I-V characteristics of the IP$_3$-dependent currents in normal high Ca^{2+} (10 mM) bathing solution and then in solutions free of divalent cations (with 2 mM EGTA), with Ca^{2+} replaced by 10 mM Ba^{2+}. As expected for authentic Icrac, Ca^{2+} is permeable, Ba^{2+} is less permeable than Ca^{2+}, and the current is blocked by Cd^{2+}. Moreover, there is an anomalous mole fraction effect that explains the large current amplitude in the absence of external Ca^{2+}. We made the same observation in 10 other cells. Our results reproduce the features of Icrac in DT40 cells previously reported by others (Kiselyov et al., 2001; Mori et al., 2002).

Features of Icrac in tyrosine kinase–deficient DT40 cells

We examined membrane currents activated by intracellular Ca^{2+} release in DT40 cell lines in which the expression of several tyrosine kinase enzymes was suppressed by homologous recombination. We studied cells that failed to express Syk, Lyn, and Btk as well as cells lacking the adaptor molecule Blnk (B cell linker protein). Typical results in cells activated with IP$_3$ loaded in the tight-seal electrode are illustrated in Fig. 3. Deletion of any one of the various tyrosine kinases alone did not eliminate the electrical response to IP$_3$ or change the quantitative feature of Icrac (Table II). In contrast, when Lyn and Syk kinases were simultaneously deleted, IP$_3$ stimulation entirely failed to elicit Icrac (Fig. 3 and Table II). That is, IP$_3$-dependent Icrac activation appears to require the normal function of either Lyn or Syk kinases.

The effect reported in Fig. 3 (and Table II) could simply be a consequence of a change in IP$_3$ sensitivity. After all, the

Table II. **Stationary current amplitude at −100 mV in wild-type and mutant DT40 cells stimulated to cause Ca²⁺ store release**

Cell type	Current amplitude			
	60 µM IP$_3$	n	1 µM TG	n
Wild type	1.29 ± 0.28	48	1.25 ± 0.40	20
blnk$^{-/-}$	0.26 ± 0.21	12	0.49 ± 0.12	6
btk$^{-/-}$	1.24 ± 0.27	11	ND	ND
lyn$^{-/-}$	1.50 ± 0.44	12	ND	ND
syk$^{-/-}$	1.63 ± 0.50	7	ND	ND
lyn/syk$^{-/-}$	0.18 ± 0.20	28	0.30 ± 0.15	9

Current amplitude is given as pA/pF ± SEM.

concentration of IP$_3$ required for the activation of Icrac is greater than that necessary to release Ca²⁺ from intracellular stores (Parekh and Penner, 1997). Furthermore, the stores that release Icrac-activating Ca²⁺ are but a specific subset of all intracellular Ca²⁺ stores in the cell (Hofer et al., 1998). We investigated the effectiveness of IP$_3$ over a large concentration range (Fig. 4) and found that IP$_3$ failed to activate Icrac even at the highest concentration tested (360 µM). Thus, failure of Syk- and Lyn-deficient cells to respond to IP$_3$ is not simply caused by a shift in the sensitivity of Icrac to IP$_3$.

Absence of Lyn and Syk specifically prevents Icrac channel gating

Failure of IP$_3$-dependent Icrac activation could arise from one or all of the following mechanisms: failure of the IP$_3$ receptor, failure of Ca²⁺ release from intracellular stores, or failure of the link between Ca²⁺ store release and Icrac activation. To distinguish among these possibilities, we investigated the effects of TG on the membrane current. TG inhibits the sarcoplasmic/ER Ca²⁺ ATPase pump and, thus, causes the release of Ca²⁺ from intracellular stores.

Fig. 5 illustrates voltage-clamped currents measured in the presence of TG in wild-type and Lyn- and Syk-deficient cells. TG activates Icrac in wild-type cells but failed to do so in the Lyn- and Syk-deficient ones (Fig. 5 and Table II). The concentration

of TG we tested, 1 µM, is ∼10-fold higher than the concentration typically sufficient to saturate the effect (Premack et al., 1994). The functional defect in Lyn- and Syk-deficient cells is not in the release of Ca²⁺.

Effect of TG on cytoplasmic Ca²⁺ in Lyn- and Syk-deficient DT40 mutant cells

In wild-type DT40 cells bathed in normal Ringer's solution, TG stimulation causes a sustained elevation of cytoplasmic free Ca²⁺ that slowly reaches a peak in 100–150 s (Fig. 6 A; Broad et al., 2001; Ma et al., 2001; Mori et al., 2002). The sustained elevation arises from the sum of two sequential events: (1) the release of Ca²⁺ from intracellular stores as a result of the TG inhibition of Ca²⁺ pumps and (2) the influx of Ca²⁺ from the extracellular space through Icrac channels activated by the initial rise in free Ca²⁺. To resolve Ca²⁺ store release from membrane Ca²⁺ influx, it is common to measure the TG-dependent Ca²⁺ response in the absence of extracellular Ca²⁺ (4 mM EGTA added to the DT40 Ringer's solution; ∼100 nM of free Ca²⁺). Under this condition, TG causes an increase in cytoplasmic Ca²⁺ (released from ER) that is smaller in amplitude and much shorter in duration than the changes observed while in the continuous presence of extracellular Ca²⁺ (Fig. 6 B).

We explored the functional role of Lyn and Syk on TG-dependent changes in cytoplasmic free Ca²⁺. In Lyn- and
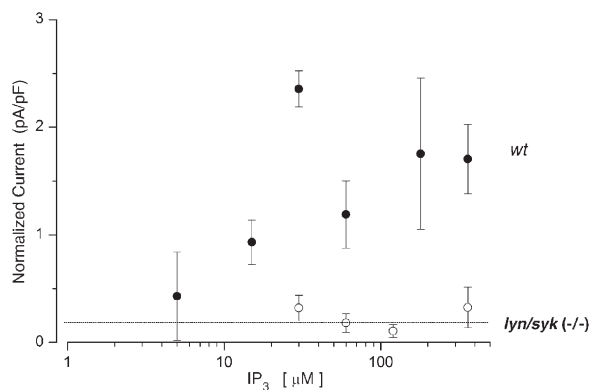
Figure 4. **Dependence of Icrac amplitude on intracellular IP$_3$ concentration in wild-type and mutant cells.** Current amplitude measured at −100 mV after cell activation. Closed circles are the mean (±SEM [error bars]) amplitude measured in wild-type (wt) cells, and open circles are data measured in Lyn- and Syk-deficient cells. Lyn- and Syk-deficient cells were not activated even at the highest IP$_3$ concentration tested.
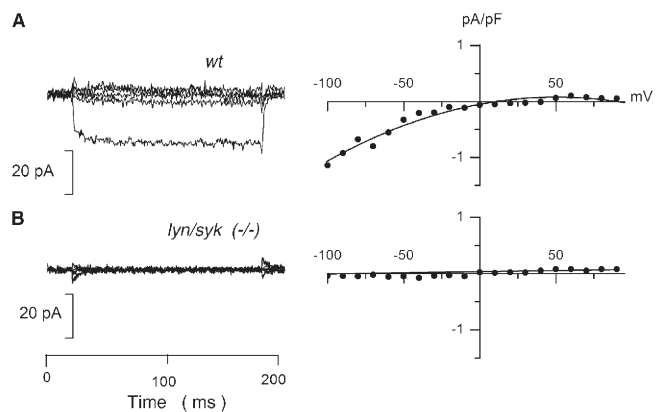
Figure 5. **Activation of Icrac in DT40 cells with 1 µM extracellular TG.** Voltage-clamped membrane currents measured in cells bathed in normal Ringer's solution. Currents activated at −100, −30, 0, 30, and 90 mV are shown. To the right of each current set is the steady-state I-V curve for that cell. (A) Wild-type (wt) cell. (B) Lyn- and Syk-deficient cell. In the absence of tyrosine kinases, Icrac current is not activated by TG.

Syk- deficient cells maintained in normal Ringer's solution, TG stimulation caused a small and transient increase in cytoplasmic free Ca^{2+} (Fig. 6 C) rather than the large and sustained change observed in normal cells (Fig. 6 A). On the other hand, the response to TG in mutant cells suspended in a Ca^{2+}-free medium (Fig. 6 D) was not different from that of normal cells (Fig. 6 B): TG caused the expected small and transient increase in free Ca^{2+}. We made similar observations in six additional experiments. That is, in Lyn- and Syk-deficient cells, the TG-dependent release of Ca^{2+} from intracellular stores is not different from that in normal cells, but the absence of tyrosine kinases causes a failure of Icrac channel activation.

The functional defect in Lyn- and Syk-deficient cells is rescued by heterologous expression of the enzymes

The failure of Icrac activation in Lyn- and Syk-deficient cells could arise specifically from the absence of tyrosine kinase activity but also from an unintended consequence of the genetic manipulation. If the failure of Icrac gating depends specifically on the expression of active kinases, restoring enzyme expression in the mutant cells should restore the wild-type–like Ca^{2+} response.

We tested this thesis by transfecting *lyn/syk*$^{-/-}$ cells with DNA constructs that command the homologous expression of the Lyn and Syk proteins alone or in combination. Furthermore, the DNA constructs commanded the expression of a reporter GFP in tandem with the kinase. This tandem expression allowed us to identify successfully transfected cells, which are expected to express the kinases, because they also fluoresced under chromatically appropriate illumination. We used an imaging instrument to measure cytoplasmic Ca^{2+}, an alternative to the mass measurement reported in the previous section and in Fig. 6, to permit us to analyze the cytoplasmic Ca^{2+} in a population consisting of more than a single cell type. We could distinguish the response of reconstituted cells (fluorescent cells expressing GFP) from that of Lyn- and Syk-deficient ones that had been identically treated but did not express the kinases.

Cells were loaded with Fura2, and the emission intensity of individual images, which were excited at 340 and 380 nm, was measured. The ratio of these intensities reports free Ca^{2+} concentration. The ratio in individual cells was averaged. The time course of the mean change in free cytoplasmic Ca^{2+} in a

cell batch is illustrated in Fig. 7 (each cell averaged). Wild-type cells were initially bathed in normal Ringer's solution. They were then locally superfused with a Ca^{2+}-free Ringer's solution (4 mM EGTA) also containing 1 µM TG. A rise in the emission intensity ratio (F340/F380) revealed the expected rise in free Ca^{2+} as a result of release from intracellular stores (Fig. 7 A). The superfusing solution was then switched to one containing the same 1 µM TG but with added Ba^{2+} (10 mM total and 8 mM of free Ca^{2+}). The addition of Ba^{2+} caused a second transient in the F340/F380 emission ratio (Fig. 7 A). The second transient arises from binding to Fura2 of Ba^{2+} that flows into the cells through the Icrac channels activated by the TG-dependent Ca^{2+} transient (Vazquez et al., 2002). Ba^{2+} was used to ensure that changes in Fura2 fluorescence arose specifically from the activation of Icrac (and associated Ba^{2+} influx), not from Ca^{2+} flux originating in unrecognized cellular sources or influx through other Ca^{2+}-permeable ion channels (see Fig. 9; compare this data with Vazquez et al., 2002).

In contrast, in Lyn- and Syk-deficient cells tested with the same protocol, TG/EGTA Ringer's solution caused the same initial transient release of Ca^{2+} from the ER observed in wild-type cells, but adding Ba^{2+} to the extracellular medium did not change Fura2 cytoplasmic fluorescence (Fig. 7 B). That is, in Lyn- and Syk-deficient cells, Icrac channels are not active and, thus, extracellular Ba^{2+} cannot flow into the cell to interact with Fura2. The same observation was made in 10 repeat experiments. Just like the findings in the measurements of cell suspensions, these results verify that lack of tyrosine kinase activity causes a loss of the linkage between Ca^{2+} store release and Icrac activation.

We measured TG-dependent Ca^{2+} changes in transiently reconstituted mutant cells that expressed tyrosine kinases 24 h after DNA transfection. In image analysis, we distinguished cells by their GFP fluorescence: GFP-negative cells were mutant *lyn/syk*$^{-/-}$ cells, whereas GFP-positive ones expressed the specific kinase of interest. In general, ~20% of the cells expressed GFP under our experimental protocol, but the level of expression varied among cells. We measured Ca^{2+} only in the cells expressing the highest level of GFP, ~5–10% of the cells. Typical results are illustrated in Fig. 7. The same observations were made in three different experiments for each transfection condition.
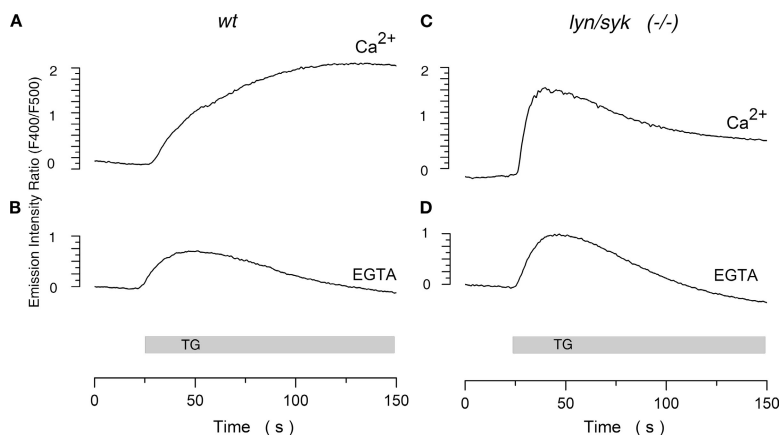
Figure 6. **Effects of 1 µM TG on cytoplasmic free Ca^{2+} in populations of normal and mutant DT40 cells.** Cytoplasmic Ca^{2+} was measured with the fluorescent Ca^{2+} indicator Indo1. An increase in the 400:500-nm emission intensity ratio reflects a rise in cytoplasmic Ca^{2+}. Cells were suspended either in normal Ringer's solution (with 1 mM Ca^{2+}) or in Ca^{2+}-free Ringer's solution (with 4 mM EGTA). (A) In wild-type (wt) cells, TG application in normal Ringer's solution caused a sustained elevation of cytoplasmic Ca^{2+}. (B) In the presence of EGTA, the TG-dependent Ca^{2+} rise was transient, and, after reaching a peak, it returned to nearly the starting value despite the continuous presence of TG. (C and D) In Lyn- and Syk-deficient cells, TG caused a nearly identical response in the presence of Ca^{2+} (C) or in its absence (D). The response was a small, transient rise in free Ca^{2+} that arises from the TG-dependent release of Ca^{2+} from intracellular stores.

Kinase-deficient cells that did not reconstitute the expression of tyrosine kinases but were nonetheless subjected to the electroporation protocol of transfection behaved indistinguishably from untreated Lyn- and Syk-deficient cells. Stimulation with TG/EGTA Ringer's solution caused a release of Ca^{2+} from intracellular stores, but Icrac was not activated, and extracellular Ba^{2+} failed to flow into the cells (Fig. 7, C–E). In contrast, the expression of kinases Lyn (Fig. 7 C) or Syk (Fig. 7 D) alone or together (Fig. 7 E) restored wild-type–like behavior in these cells. TG caused intracellular Ca^{2+} release, which activated Icrac channels that, in turn, sustained Ba^{2+} influx.

Examination of data in Fig. 7 reveals that the expression of tyrosine kinases restored Icrac gating, but it should be noted that the Ba^{2+}-dependent fluorescence changes are not quantitatively similar to the response in wild-type cells and, in fact, differed among the various transfected cell batches tested. This is not surprising because we could not control the level of expression of the kinases in the transfected cells, and, moreover, there is no reason to expect that these levels would be identical to those in wild-type cells or amid different cell batches. Nonetheless, restoring kinases in Lyn- and Syk-deficient cells always rescued the cell phenotype, indicating that functional defects in the deficient cells arise specifically from the lack of these kinases. As we observed in electrical studies of mutant cell lines (Fig. 3), the presence of either Lyn or Syk alone is sufficient to obtain normal function.

Mechanisms of Lyn and Syk action

Although the detailed molecular mechanisms whereby Lyn and Syk function to link Ca^{2+} release to Icrac gating remain to be determined, we tested two possibilities: (1) that these mechanisms act on the events linking Ca^{2+} release and channel gating and (2) that the enzymatic activity of the kinases change in the course of Ca^{2+} store release and/or channel gating.

A parsimonious thesis suggests that kinases act on the molecular events that link Ca^{2+} release and channel gating. However, it can be argued that the action of kinases is not direct but arises from long-term effects of enzyme activity on events such as gene expression or cellular protein trafficking. To assess whether the kinase action is immediate and direct or not, we tested the effectiveness of drugs known to act as specific tyrosine kinase inhibitors. If the role of kinase activity is direct, drug treatment should have the same effect on TG-dependent Icrac activation as on the genetic suppression of enzyme expression.

We tested the effectiveness of two well-established kinase inhibitors: LavendustinA, a specific tyrosine kinase inhibitor that does not distinguish among enzyme types (Onoda et al., 1989; Ping et al., 1999), and PP2, a selective inhibitor of the Src family tyrosine kinase. We first used an electrophysiological assay to test the effect of LavendustinA on TG-dependent Icrac activation. Cells were treated with 10 µM LavendustinA starting 10 min before the functional assay and throughout the assay. Electrophysiological data in Fig. 8 are typical of experiments that were repeated five times. In normal cells, TG caused activation of an inward current at −90 mV that developed slowly and reached its maximum steady amplitude ∼60–100 s after initiating TG stimulation (Fig. 8 A, inset). The I-V curve of this TG-dependent current was measured by taking the difference in I-V curves before TG stimulation (time 0 data point) and 85 s after initiating

Figure 7. **Restoration of TG-dependent Icrac activation by Lyn and/or Syk homologous expression in *lyn/syk*$^{-/-}$ cells.** Cytoplasmic Fura2 emission fluorescence intensity ratio at 340 and 380 nm was measured in individual cells and averaged. (A) Wild-type cells stimulated by 1 µM TG in a Ca^{2+}-free Ringer's solution (with 4 mM of added EGTA) demonstrated a transient release of Ca^{2+} from the ER stores. Switching to an extracellular solution containing Ba^{2+} added to the EGTA-containing Ringer's solution (10 mM Ba^{2+} added, yielding 8 mM of free Ca^{2+}) caused a change in Fura2 fluorescence as a result of Ba^{2+} influx through activated Icrac channels (mean of 42 cells). (B) Lyn- and Syk-deficient cells. TG caused the release of intracellular Ca^{2+} stores, but the addition of extracellular Ba^{2+} did not cause changes in intracellular Fura2 fluorescence because Ba^{2+} influx does not occur in the absence of active Icrac channels (mean of 19 cells). Panels on the right illustrate results from measurements in Lyn- and Syk-deficient cells reconstituted to express Lyn or Syk alone or together. Because the heterologous protein was in fusion with GFP, cells in a field of view were identified as kinase expressing and GFP positive (closed circles) or as *lyn/syk*$^{-/-}$ and GFP negative (open circles). The response of Lyn- and Syk-deficient cells is the same in all panels (C, mean of 35 cells; D, 20 cells; E, 25 cells). TG causes intracellular Ca^{2+} release, but Ba^{2+} cannot enter through closed Icrac channels. On the other hand, the successful expression of tyrosine kinases (C, Lyn alone, mean of nine cells; D, Syk alone, three cells; E, both, three cells) allows Icrac activation by released Ca^{2+}, and, thus, changes in Fura2 fluorescence are observed in these cells when the bathing solution is switched to one containing Ba^{2+}. In E, the dotted line identifies the moment Ba^{2+} was first added to the bathing solution. It corresponds to the transition from gray to black in the horizontal bar.
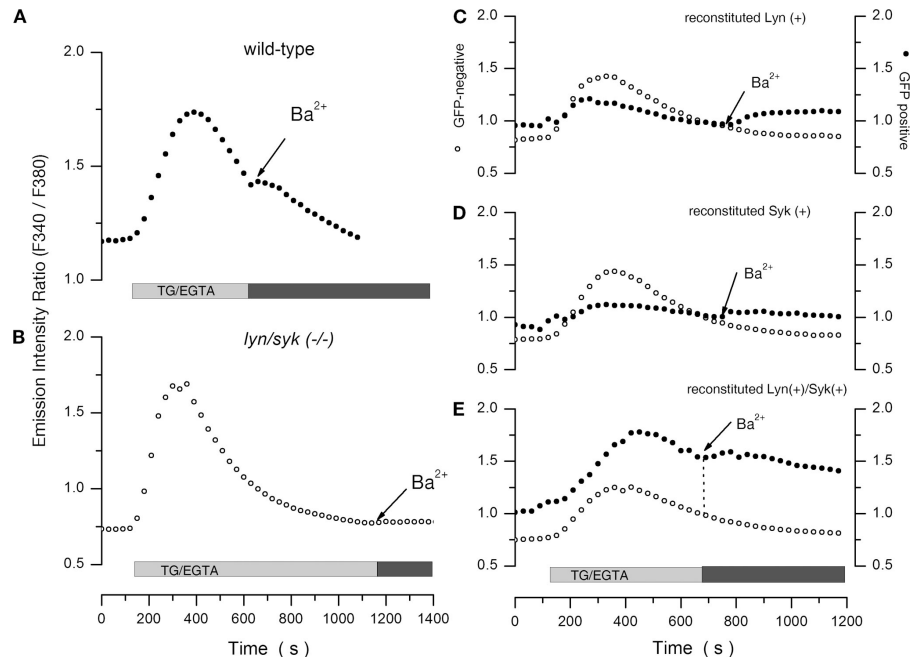
TG stimulation (time 165 s data point). The difference in the I-V curve thus computed is typical of Icrac (Fig. 8 A). In contrast, in LavendustinA-treated cells, TG failed to activate an inward current at −90 mV (Fig. 8 B, inset). In three different LavendustinA-treated cells, we followed the current for up to 20 min after initiating TG stimulation and did not observe any substantial activation. Also, in the presence of LavendustinA, there was no difference in the I-V curves measured at time 0 and at 165 s (Fig. 8 B).

Having demonstrated that LavendustinA specifically prevents TG-dependent Icrac activation, we also tested the drug effect in a single-cell Ca^{2+} imaging assay of Fura2-loaded cells. As illustrated in Fig. 7 A, in wild-type cells and in the absence of extracellular Ca^{2+}, TG causes a transient increase in cytoplasmic Ca^{2+} because of the cation release from intracellular stores. If Ba^{2+} is then added to the extracellular medium, the cation flows into the cell only if Icrac channels have been activated and causes a second, prominent increase in the Fura2 emission intensity ratio. In contrast, in Lyn- and Syk-deficient cells, Icrac is not activated, and, therefore, extracellularly added Ba^{2+} does cause any changes in Fura2 fluorescence (Fig. 8 C). The same phenotype is observed in LavendutinA-treated cells: TG causes an initial rise in cytoplasmic Ca^{2+}, but the addition of extracellular Ba^{2+} does not cause any change in the Fura2 emission intensity (Fig. 8 D).

We tested the effect of PP2, a potent and specific inhibitor of the Src kinase family (that is, a specific inhibitor of Lyn), on TG-dependent Ca^{2+} fluxes in suspensions of cells loaded with the Ca^{2+} indicator Indo1 (Fig. 9). Again, in wild-type cells, 1 μM TG delivered in the presence of EGTA caused a transient

increase in cytoplasmic free Ca^{2+}, which was followed by a much larger and sustained change in concentration when Ca^{2+} was added to the extracellular medium (Fig. 9 A). In Lyn- and Syk-deficient cells, TG caused the initial rise in cytoplasmic Ca^{2+}, but, because Icrac channels are not activated, the added external Ca^{2+} caused only a modest change in cytoplasmic free Ca^{2+} when compared with the normal cells (Fig. 9 B). Treatment of wild-type cells with 20 μM PP2 caused a functional phenotype that was indistinguishable from that of the Lyn- and Syk-deficient cells. In PP2-treated cells, TG added in a medium free of divalent cations caused a transient increase in cytoplasmic Ca^{2+}, but the addition of Ca^{2+} to the extracellular medium did not cause any further changes in cytoplasmic free Ca^{2+} (Fig. 9 C). These pharmacological findings together with the results of genetic manipulations demonstrate that Lyn activity is required for Icrac gating even if Syk activity is unchanged. That is, the tyrosine kinases are required, and Lyn (and other Src kinases) is likely upstream of Syk in this pathway.

Biochemical assay of Lyn and Syk phosphorylation activity

We measured the level of phosphorylation of Lyn and Syk kinase proteins. This autophosphorylation is a parameter that can reflect kinase activity. To increase sensitivity, all tyrosine-phosphorylated proteins in cell lysates were first immunoprecipitated with panspecific phosphotyrosine mAbs. These immunoprecipitates were then probed in a Western blot using antibodies that bound to specific phosphotyrosine residues in Lyn and Syk (Fig. 10 A).
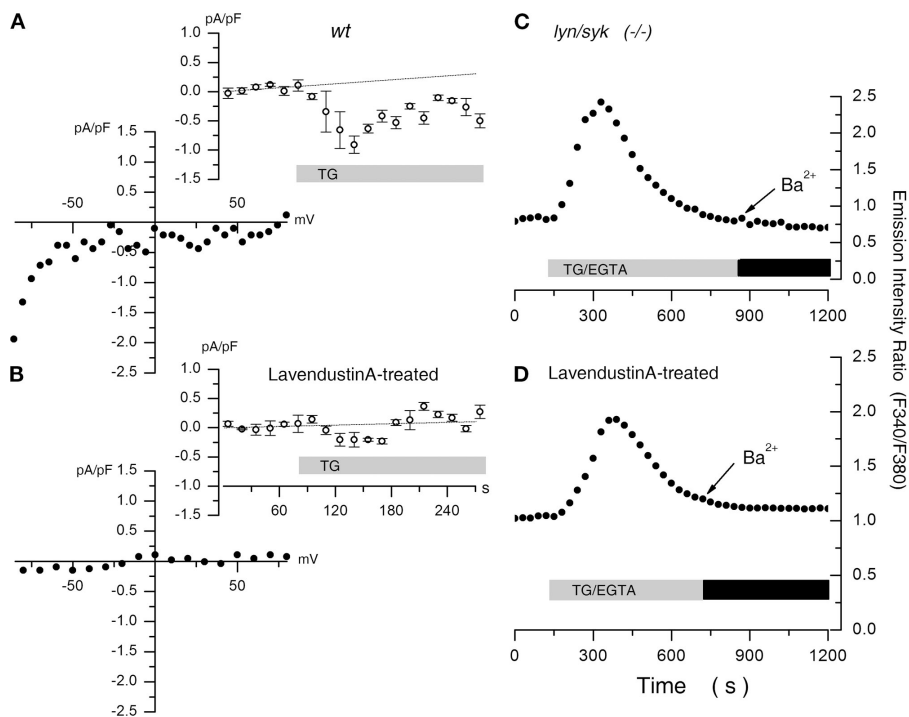

Figure 8. **The specific tyrosine kinase inhibitor LavendustinA blocks the activation of Icrac in wild-type DT40 cells.** (A and B) Electrophysiological assay. Membrane voltage was held at 0 mV, and the difference in current amplitude in response to −90-mV steps was measured repeatedly every 3 s and box car averaged over three adjacent data points. In the graph, time 0 is the moment whole cell mode was first achieved. 90 s thereafter, the cell bathing solution was switched to one containing 1 μM TG. (A) In a normal cell, TG slowly activated an inward current that reached a final, stationary value ~60 s after TG superfusion began (inset). The I-V curve of the TG-dependent current was measured as the difference in I-V curves acquired at time 0 s and at 85 s after initiating TG superfusion. This I-V curve is typical of Icrac. (B) TG, in contrast, did not cause any current change in cells treated with LavendustinA (inset). Because there are no TG-dependent currents in LavendustinA-treated cells, the difference in I-V curves acquired at time 0 and at 85 s after initiating TG superfusion is essentially flat. (C and D) Ca^{2+} imaging assay. (C) In Lyn- and Syk-deficient cells, stimulation with 1 μM TG in a Ca^{2+}-free Ringer's solution (with 4 mM EGTA) caused a rise in intracellular Ca^{2+} (increase in Fura2 fluorescence F340/F380 emission intensity), but adding Ba^{2+} to the EGTA-containing Ringer's solution (10 mM Ba^{2+} added, yielding 8 mM of free Ca^{2+}) to the extracellular medium did not cause further changes in Fura2 fluorescence (mean of 45 individual cells). (D) Wild-type cells were incubated for 10 min with 10 μM LavendustinA and assayed in the continuing presence of the drug. These drug-treated cells exhibit the same functional behavior as Lyn- and Syk-deficient ones: Icrac is not activated, and Ba^{2+} added after TG stimulation does not cause the enhancement in Fura2 emission intensity observed in wild-type cells. Error bars represent SEM.
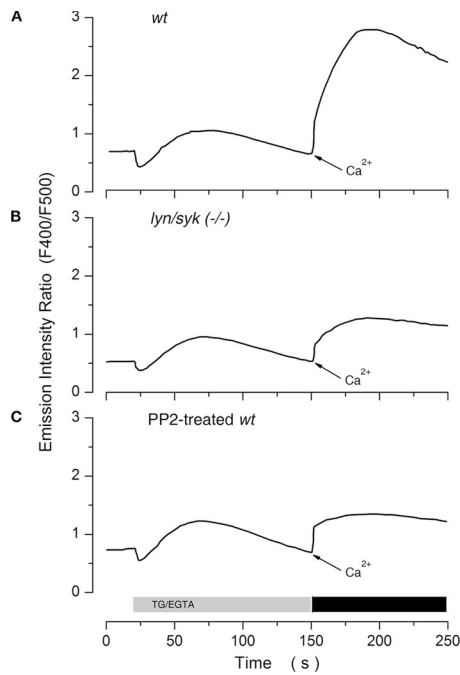
Figure 9. **The specific Src tyrosine kinase inhibitor PP2 blocks the activation of Icrac in wild-type DT40 cells.** Cytoplasmic free Ca^{2+} measured in a suspension of cells loaded with Indo1. (A) Normal cells suspended in Ca^{2+}-free Ringer's solution (4 mM EGTA) respond to stimulation by 1 μM TG with a small, transient increase in free Ca^{2+}. Addition of external Ca^{2+} to the EGTA-containing Ringer's solution (5 mM Ca^{2+} added, yielding 1 mM of free Ca^{2+}) causes a large increase in cytoplasmic Ca^{2+} as a result of cation influx through activated Icrac channels. (B) Lyn- and Syk-deficient cells. In response to 1 μM TG in a Ca^{2+}-free Ringer's solution, there is a small, transient increase in Ca^{2+} similar to that in wild-type (wt) cells. The addition of extracellular Ca^{2+} causes a small additional increase in free Ca^{2+} that is smaller in extent than that observed in wild-type cells. (C) Wild-type cells treated with 20 μM PP2. The functional behavior of these cells is indistinguishable from the Lyn- and Syk-deficient ones. In the absence of extracellular Ca^{2+}, TG causes a small and transient Ca^{2+} release from intracellular stores. Icrac is not activated, and, therefore, the addition of extracellular Ca^{2+} does not cause the large and sustained increase in free Ca^{2+} observed in untreated normal cells.

TG stimulation had different effects on the two enzymes. Syk exhibited a low level of phosphorylation before stimulation, which was not detectably changed by TG. In contrast, Lyn had a low level of phosphorylation before stimulation, and TG increased this level ∼2.5-fold. As a control, we used immunoprecipitates isolated from Lyn- and Syk-deficient cells, and, as expected, there was no detectable signal for either of these kinases (Fig. 10 A). Also, we measured the phosphorylation of these kinases in BCR-stimulated cells, and, consistent with previous observations (Mizuguchi et al., 1992; Ma et al., 2001), we observed a stimulated phosphorylation of approximately sevenfold for each kinase.

Expression levels of STIM1 protein and of STIM1 and Orai1 mRNA in Lyn- and Syk-deficient cells

Recent experiments have demonstrated that two membrane-associated proteins, STIM1 (Liou et al., 2005; Roos et al., 2005; Zhang et al., 2005) and Orai1 (Feske et al., 2006, Vig et al., 2006b), participate in the events linking Ca^{2+} store release to

Icrac channel activation in lymphocytes. It is possible, then, that the effects of Lyn and Syk arise from their action on these proteins. Future work must explore whether these proteins are phosphorylated and what role tyrosine kinases might play. In this study, we tested the possibility that Syk and Lyn act as regulators of the expression of either or both of these proteins. We tested this thesis by assaying the protein expression level of STIM1 and the mRNA expression level of both STIM1 and Orai1. We find that none of these is detectably different in wild-type and mutant cells.

STIM1 protein levels were measured in Western blots. Individual lanes in SDS-PAGE were loaded with the same total protein amount. The relative amount of protein identified with an STIM1 antibody was assessed by chemiluminescence. Samples from wild type and the following mutants were run alongside each other in the same gel: $lyn^{-/-}$, $syk^{-/-}$, $lyn/syk^{-/-}$, $blnk^{-/-}$, and $IP_3^{-/-}$ receptor (Fig. 10 B). The expression levels of tubulin in each sampled lane were also measured to confirm that the amount of protein loaded in each lane was essentially the same (Fig. 10 B). There was no detectable difference in the level of STIM1 protein between wild type and the various mutant cells tested.

mRNA levels of STIM1 and Orai1 were assayed with semiquantitative RT-PCR. Total cell RNA was used to synthesize cDNA, which, in turn, was amplified using PCR. The amount of gene-specific DNA produced under identical reaction conditions was compared for STIM1 and Orai1-specific primers in wild type and in the following mutants: $lyn^{-/-}$, $syk^{-/-}$, $lyn/syk^{-/-}$, $blnk^{-/-}$, and $IP_3^{-/-}$ receptor. PCR products were loaded at various dilutions into the lanes of an agarose gel and separated by size. The level of β-actin mRNA was also assessed in each of the cell samples. The amount of DNA in each well was quantified by the intensity of fluorescence in images of ethidium bromide–stained gels (Fig. 10 C). There was no detectable difference in the STIM1 and Orai1 mRNA levels between wild type and the various mutant cells tested.

Discussion

In B lymphocytes, binding of antigen or antireceptor antibody to the BCR complex recruits and activates tyrosine kinases as part of the events that lead to the production of IP_3 (Rawlings, 1999; Wollscheid et al., 1999; for reviews see Kurosaki, 2000; Wienands, 2000). Results presented in the current study indicate that these kinases also play a role in the link between the IP_3-dependent release of Ca^{2+} from ER intracellular stores and activation of the Icrac ion channels in the plasma membrane. We compared the electrophysiological features of Icrac and changes in free cytoplasmic Ca^{2+} between wild-type and Lyn- and Syk-deficient DT40 cells and found that cells simultaneously lacking Lyn and Syk tyrosine kinases fail to activate Icrac after the release of Ca^{2+} stores. Interestingly, the genetic deletion of either enzyme alone did not prevent Icrac activation, revealing redundancy in the biological function of these kinases in this response. The physiological effects on Icrac and cytoplasmic Ca^{2+} flux of pharmacological blockers of these enzymes leads us to suggest that the enzymes may operate in a sequential cascade with the
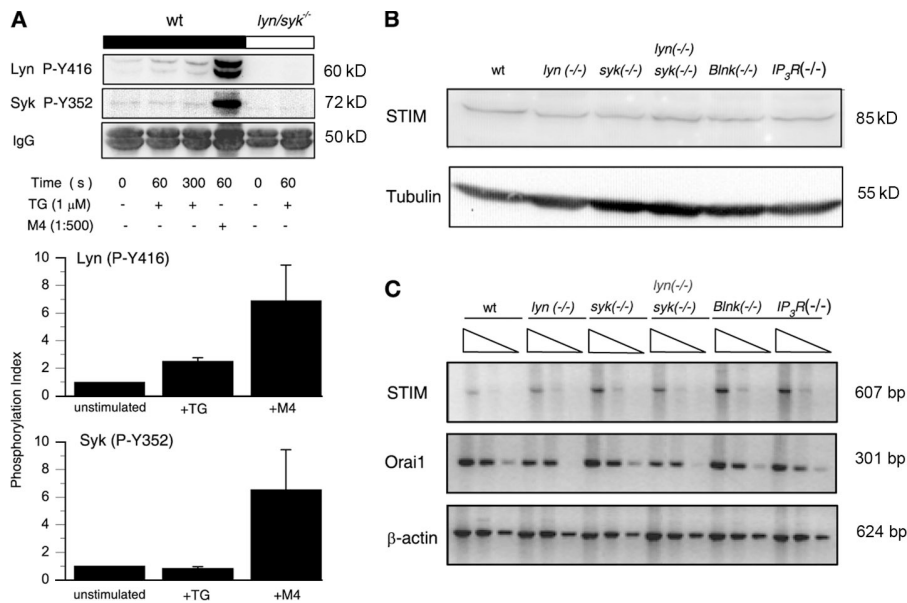
Figure 10. **Biochemical analysis of Lyn and Syk autophosphorylation activity in wild-type and mutant cells.** Analysis of the expression of STIM1 and Orai1 in wild-type and mutant cells. (A) BCR- and TG-stimulated Lyn/Syk activity in DT40 cells. Wild-type (wt) or Lyn- and Syk-deficient cells were stimulated with anti-BCR antibody (M4) or with TG. Western blots of immunoprecipitates of tyrosine phospho-proteins isolated from the cells before and 60 or 300 s after TG or the M4 stimulation (as labeled). The same blot was successively probed with antibodies specific for the activation loop in Syk (P-Y352) or Src (P-Y416) kinases. The extent of antibody binding was quantified in relative units of activity (phosphorylation index). The levels of IgG are also shown to demonstrate that the total amount of tyrosine-phosphorylated protein in each lane is similar. The bar graphs are means ± SEM (error bars) of the phosphorylation index in five different experiments measured from the absolute values of gray level (at 10-bit resolution) in the original blots. The images displayed for each of the various antibodies tested were independently adjusted with respect to brightness and contrast to bring forth the individual bands (Photoshop [Adobe] at 8-bit gray level resolution). Therefore, visual perception of the band intensity in the images is skewed and does not necessarily match the analytical bar graph. (B) Chemiluminescent image of a Western blot of wild-type and mutant cells assayed for the protein level of STIM1 and tubulin. SDS-PAGE–separated total protein samples were blotted and subsequently identified with specific primary antibodies. The level of expression was determined by the gray level of chemiluminescent images of the identified protein bands. Within the resolution of the technique, STIM1 protein levels are not different in wild-type and mutant cells. (C) Images of ethidium bromide–stained DNA bands in an agarose gel. DNA was obtained by PCR amplification of cDNA using primers specific for STIM1, Orai11, and β-actin. PCR reactions were performed in serially diluted (1:5) samples of the same starting cDNA. After identical PCR reactions, DNA products were size separated by gel electrophoresis, and the gel was stained with ethidium bromide. DNA levels were assessed by the gray level in the images. Within the resolution of the technique, STIM1 and Orai11 mRNA levels are not different in wild-type and mutant cells.

Src family enzyme (Lyn) upstream from Syk. The failure to activate Icrac in the Lyn- and Syk-deficient cells reflects that protein phosphorylation is a required event in the mechanism that couples the emptying of Ca^{2+} stores to channel activation or in the function of the channels themselves. These alternatives cannot now be unequivocally discerned.

There are no previous studies on the electrical properties of lymphocytes with the genetically suppressed expression of tyrosine kinases. However, the hypothesis that tyrosine kinases may play a role in the link between Ca^{2+} store release and Icrac activation has been proposed previously (Lee et al., 1993; Sargeant et al., 1993a,b; Rosado et al., 2000). Lymphocytes of mice in which the Btk-related Itk tyrosine kinase is knocked out respond to T cell receptor activation with a normal release of intracellular Ca^{2+} stores, but Icrac activation by TG is less than in wild-type animals (Liu et al., 1998). In addition to observations in animals subjected to genetic manipulation, a possible role for tyrosine kinases in lymphocyte Ca^{2+} transduction paths has been suggested by experimental observations of some effects of the pharmacological inhibition of tyrosine kinase activity (Whisler et al., 1991; Mizuguchi et al., 1992; Schieven et al., 1993; Nagao et al., 1996).

Currently, the mechanisms that couple Ca^{2+} store release to Icrac gating fall into two main categories: (1) physical coupling mechanisms propose that activation of the IP_3 receptors are directly linked through conformational changes to the opening of Icrac channels. An alternative form of physical coupling, the vesicle fusion hypothesis proposes a fusionlike event between intracellular vesicles and the plasma membranes that delivers Icrac channels or their activators to the plasma membrane. Vesicle fusion is mediated by SNARE proteins. (2) Messenger mechanisms propose that the released Ca^{2+} is detected by particular cytoplasmic Ca^{2+} sensor molecules that, in turn, gate channel activity.

The direct coupling hypothesis was developed to explain findings that Icrac fails to occur after pharmacological treatments expected to disrupt cytoskeletal elements (for example, cytochalasin D [Patterson et al., 1999], calyculin A [Patterson et al., 1999], 2APB [Patterson et al., 1999], or clostridium C3 transferase injection [Yao et al., 1999]). Direct coupling supposes that molecular receptors in the ER membranes, IP_3 receptors, or ryanodine receptors are linked to Icrac activation through conformational changes. In lymphocytes in particular, this hypothesis is unlikely because mutant DT40 cells lacking all IP_3 receptor isoforms exhibit normal TG-activated Icrac (Prakriya and Lewis, 2001) and ryanodine receptor knockout animals have normal T cell activation (Takeshima et al., 1996).

The vesicle fusion hypothesis (for review see Rosado et al., 2005) was developed to explain the fact that interference with the function of all or even some of the various proteins that constitute the SNARE complex can block TG-dependent Ca^{2+} elevation. Although it is evident that SNARE protein can alter the cell's Ca^{2+} response, it remains questionable whether their specific activation by IP_3-linked events is required in the course of normal events linking Ca^{2+} store release and Icrac gating (Scott et al., 2003).

Recent studies have identified two novel proteins, STIM1 and Orai1, that participate in the signaling between store Ca^{2+}

release and Icrac activation (Zhang et al., 2005; Feske et al., 2006; Peinelt et al., 2006). They are both integral membrane proteins located either in the ER membrane (STIM1) or in the plasma membrane (Orai1). Their simultaneous coexpression enhances Ca²⁺-dependent Icrac gating. These may be the first identified constituents of a larger family of proteins involved in the linkage between Ca²⁺ store release and channel gating. The results we present here firmly indicate that the link between the release of Ca²⁺ stores and Icrac activation in B cells also involves protein phosphorylation catalyzed by cytoplasmic tyrosine kinases. The target of phosphorylation remains to be identified in future work; it could be STIM1, Orai1, or other proteins yet to be discovered. However, we have demonstrated that kinase activity does not affect the expression levels of STIM1 or Orai1.

We emphasize that our results suggest that the state of phosphorylation of a target protein is important, but we have no evidence, nor do we suggest that Ca²⁺ sensing or channel gating is mediated by phosphorylation. We assayed kinase autophosphorylation as an index of enzymatic activity. Our biochemical results reveal that the activity of one of the critical kinases (Syk) does not change with Ca²⁺ release, whereas the other (Lyn) changes only by a small extent and with a slow time course. We propose that phosphorylation is required as a tonic signal that sustains the normal function of its target protein rather than a phasic signal activated in the course of Ca²⁺ release, Ca²⁺ sensing, or channel gating.

Materials and methods

Materials

IP₃, TG, ionomycin, fibronectin, antiphosphotyrosine antibody 4G10, LavendustinA, and PP2 (4-amino-5-(4-chlorophenyl)-7-(t-butyl)pyrazolo[3,4-d] pyrimidine) were obtained from Calbiochem. The STIM1 antibody was purchased from BD Biosciences. M4, an anti-DT40 BCR chain mAb, was prepared as described previously (Zhao and Weiss, 1996). Indo1–acetoxy-methyl and Fura2–acetoxy-methyl were obtained from Invitrogen. Phospho-Src family (P-Y416) and phospho–Zap-70 (P-Y319)/Syk (P-Y352) antibodies were purchased from Cell Signaling Technology. pLynGFP and pSykEGPF, which were gifts from A. Defranco (University of California, San Fransisco, San Fransisco, CA), are vectors that promote the expression of Lyn/GFP or Syk/EGFP proteins.

Cell lines and solutions

DT40 cells were cultured at 37°C in 5% CO₂ in RPMI 1640 with 10% FCS, 1% chicken serum, and 2 mM glutamine. Generation of every cell mutant DT40 cell line has been reported previously: *lyn/syk⁻/⁻* and *btk⁻/⁻* (Takata and Kurosaki, 1996), *lyn⁻* and *syk⁻* (Takata et al., 1994), and *bln⁻* (Ishiai et al., 1999). Mutant cells were transfected with pLynGFP or pSykEGPF by electroporation and grown for 24 h after transformation before Ca²⁺ imaging experiments.

DT40 Ringer's solution consisted of 145 mM NaCl, 2.8 mM KCl, 10 mM CsCl, 10 mM CaCl₂, 2 mM MgCl₂, 10 mM glucose, and 10 mM Hepes-NaOH, pH 7.4. Tight-seal electrodes were filled with a quasi-intracellular solution of the composition 145 mM Cs glutamate, 8 mM NaCl, 1 mM MgCl₂, 2 mM MgATP, 10 mM EGTA, and added Ca²⁺ to yield 90 nM of free Ca²⁺. Free Ca²⁺ in the presence of the various Ca²⁺-binding molecules was calculated using WinMaxC.

In some experiments, we tested the ion selectivity of Icrac by measuring the current in an extracellular solution consisting of 150 mM Na methane-sulfonate, 10 mM Hepes, pH 7.4, and 2 mM EGTA with varying amounts of Ca²⁺, Ba²⁺, and Cd²⁺. Osmotic pressure was 300 mosM (adjusted with glucose). In only these experiments, we filled the tight-seal electrode with 128 mM Cs glutamate, 3.16 mM MgCl₂, and 10 mM EGTA and added Ca²⁺ to yield 90 nM of free ion.

Electrophysiological studies in single cells

Cells were washed free of incubation medium and resuspended at ∼10⁵/ml in Ringer's solution. 200 µl of the cell suspension was applied onto a fibronectin-coated glass coverslip that formed the bottom of a recording chamber held on an upright microscope (Diaphot; Nikon) equipped with differential interference contrast optics. The cells were maintained at room temperature and continuously superfused with oxygenated recording solution. Drugs of interest were tested by adding them to the superfusing solution.

We measured membrane currents under voltage clamp at room temperature in the whole cell mode configuration using tight-seal electrodes produced from aluminosilicate glass (1.5 × 1.0 mm [outer diameter × inner diameter]; 1724; Corning). We used a patch-clamp amplifier (Axopatch 1B; Axon Instruments, Inc.), with which we compensated (and measured) membrane capacitance but not series resistance. Analogue signals were low-pass filtered below 1 KHz with an 8-pole Bessel filter (Frequency Devices) and digitized online at 3 KHz with FastLab (Indec Systems) or pClamp (Axon Instruments, Inc.). Bath was grounded through an Ag/AgCl electrode connected to the solution via a 1-M KCl agar bridge to avoid shifts in electrode potential as solutions changed.

Two voltage command protocols were used, steps or ramp, depending on the purpose of the experiment. In the voltage step protocol, voltage was held at 0 mV and was stepped for 160 ms to values between −100 and 90 mV in 10-mV increments. This protocol was applied immediately after attaining whole cell mode and before adding any stimulant. The I-V curve thus generated was defined as the cells leak. Cells were chemically stimulated, and the voltage step protocol was executed again 2 min thereafter. The I-V curves are corrected for nonspecific electrical leakage. This correction was carried out by measuring the I-V curve before chemical subtraction and subtracting these data from the I-V curve measured after stimulation. Continuous I-V functions were fit to discrete data points with a second degree polynomial using nonlinear least-square minimization algorithms (Origin; Microcal).

To investigate the time course of Icrac development and the effects of LavendustinA, we used a voltage ramp protocol. Voltage was held at 0 mV, and acquisition epochs were repeated continuously at 3-s intervals starting immediately after attaining whole cell mode and for as long as 25 min. In each acquisition epoch, voltage was initially stepped to −100 mV for 100 ms, and then a linear voltage ramp was applied between −100 and 100 mV over 100 ms before returning to −100 mV for another 100 ms. To determine the time course of Icrac development, we measured in each of the successive epochs the difference between the mean current amplitude at 0 mV and the amplitude 90 ms after stepping to −90 mV. The cell's I-V curve was measured directly from the ramp data.

Measurement of cytoplasmic free Ca²⁺ in cell suspensions

To load, Indo1 was loaded into cells by incubating ∼3 × 10⁶ cells/ml in RPMI 1640 with 10% FBS and 3 µM Indo1–acetoxy-methyl (Invitrogen) for 1 h at 37°C. The cells were then washed three times at room temperature with a DT40 Ringer's solution consisting of 125 mM NaCl, 5 mM KCl, 1 mM CaCl₂, 0.5 mM MgCl₂, 1 mM Na₂HPO₄, 11 mM glucose, and 25 mM Hepes, pH 7.4, with 0.1% wt/vol BSA added. The last cell pellet was maintained on ice until just before measurements. To measure Ca²⁺, ∼2 × 10⁶ Indo-loaded cells/ml were suspended in DT40 Ringer's solution with BSA and maintained at 37°C in a stirred cuvette in a fluorimeter (F-4500; Hitachi). Fluorescence emission intensity ratio at 400 and 500 nm (F400/F500) was measured continuously and assessed in response to stimulants injected into the stirred cuvette.

Single-cell Ca²⁺ imaging

In single-cell studies, we used the fluorescent dye Fura2 in a modified epifluorescent microscope. Cells were loaded by incubation in Fura2–acetoxy-methyl (Invitrogen) as described above for Indo1–acetoxy-methyl. Immediately after the last wash, cells were suspended in DT40 Ringer's solution at ∼10⁵ cells/ml, and 200 µl was deposited on an imaging chamber held on the stage of the inverted microscope. The bottom of this chamber was a glass coverslip coated with 0.1 mg/ml poly-L-lysine, to which cells adhered. Cell fluorescence was excited at either 340 or 380 nm (narrow band interference filters selected with a rotating wheel; Sutter Instrument Co.). Cells were observed using a 20× 0.75 NA Fluor objective (Nikon), and images were captured through a 510 ± 40-nm bandpass optical window using a cooled high resolution CCD camera (MicroMAX 1300; Roper Scientific), an ST133 controller, and WinView32 software (Roper Scientific). Image pairs at 340 or 380 nm were acquired for 5 s each, separated by 0.5 s from one another. Image pairs were repeated at 30-s intervals over

20 min. To minimize fluorophore bleaching, an electronic shutter (LPS25; Vincent Associates) was used to restrict cell illumination to the time of image acquisition.

In off-line analysis (Simple PCI software; Compix, Inc.), we selected images of individual cells that met three criteria: diameter within 10% of the population mean, low resting cytoplasmic Ca^{2+}, and no detectable movement or loss of focus over the time course of the measurements. The mean gray level (at 10 bit resolution) of the emission intensity at 340 and 380 nm was measured for each selected cell at each time point and averaged over the cell population. Absolute cell emission intensity was calculated by subtracting the mean intensity of the background.

Single-cell superfusion

The cell-bathing Ringer's solution in the microscope imaging chamber was exchanged throughout an experimental measurement at a rate of ~0.5 ml/min. In addition, the medium specifically bathing cells in a selected field of view was controlled by local superfusion with solutions flowing from a 300-μm–inner diameter polyimide capillary tubing (PT Technologies) placed with its tip in the same plane as the cells and ~300 μm away. This superfusing medium rapidly (≤200 ms) changed in the course of cytoplasmic Ca^{2+} level measurements. The polyimide tubing was the exit port of micromanifold (MM-6; Warner Instruments) that allowed selection among six possible solutions. The identity and duration of flow of the superfusing solution were controlled with electronic switch valves (MPS-2; WPI Instruments).

Tyrosine phosphorylation assay

1.0×10^8 DT40 cells were suspended in RPMI, stimulated by the addition of TG or M4, and sampled at different time points after stimulation. Cells were spun, lysis buffer was added, cells were spun again, and the supernatant was collected. 4G10 antibody was added to the supernatant and incubated for 1 h at 4°C on a rocker. Protein G beads were then added, and the suspension was incubated for an additional 2 h at 4°C. The beads with bound tyrosine-phosphorylated proteins were washed four times with lysis buffer and dissolved in standard SDS sample buffer with DTT. Proteins were separated in gradient 5–15% SDS-PAGE, blotted onto nitrocellulose, and reacted with antibodies. The reaction product was located on the blot with secondary antibodies linked to HRP and reacted with the chemiluminescent substrate Luminol. Within 1 min, luminescent images were acquired with a cooled high resolution CCD camera (MicroMAX 1300; Roper Scientific). In off-line image analysis (Simple PCI software; Compix), we measured the absolute gray level of each luminescent band.

Expression levels of STIM1 and Orai1

Expression levels of STIM1 protein were assessed in a Western blot using anti-STIM1 primary antibody and a secondary antibody linked to HRP. SDS-PAGE lanes were loaded with 200 μg of protein and transferred onto a nitrocellulose membrane, which was then incubated for 2 h at room temperature with the primary antibody dissolved in 3% (wt/vol) BSA in Tween-PBS. After exhaustive washing, the membrane was further incubated with the secondary antibody for 1 h at room temperature. The extent of antibody binding was assessed using chemiluminescence (PerkinElmer).

The expression levels of STIM1 and Orai1 mRNA were assessed with semiquantitative RT-PCR. Total RNA from wild-type and mutant DT40 cells was purified using the RNeasy kit (QIAGEN). First-strand cDNA was produced using the Superscript III first-strand synthesis system (Invitrogen). Serial 1:5 dilutions of the cDNAs were then used in PCR reactions using the primers of the following sequences: STIM1, forward (GGGACTGTGCTGAAG-ATGACAGACCG) and reverse (TCCTTGGCCACCAGGAGCTGCTTCTC); Orai1, forward (GGCTTCGCCATGGTGGCCATGGTAGA) and reverse (TCACCCAACACAGCAACACCACCTC); and β-actin, forward (CCCTCC-CCCATGCCATCCTC) and reverse (CCGGTTTAGAAGCATTTGCGG).

References

Alvarez, J., M. Montero, and J. Garcia-Sancho. 1992. Cytochrome P450 may regulate plasma membrane Ca2+ permeability according to the filling state of the intracellular Ca2+ stores. *FASEB J.* 6:786–792.

Berridge, M.J., M.D. Bootman, and H.L. Roderick. 2003. Calcium signalling: dynamics, homeostasis and remodelling. *Nat. Rev. Mol. Cell Biol.* 4:517–529.

Bird, G.S., and J.W. Putney Jr. 1993. Inhibition of thapsigargin-induced calcium entry by microinjected guanine nucleotide analogues. Evidence for the involvement of a small G- protein in capacitative calcium entry. *J. Biol. Chem.* 268:21486–21488.

Broad, L.M., F.J. Braun, J.P. Lievremont, G.S. Bird, T. Kurosaki, and J.W. Putney Jr. 2001. Role of the phospholipase C-inositol 1,4,5-trisphosphate pathway in calcium release-activated calcium current and capacitative calcium entry. *J. Biol. Chem.* 276:15945–15952.

Csutora, P., Z. Su, H.Y. Kim, A. Bugrim, K.W. Cunningham, R. Nuccitelli, J.E. Keizer, M.R. Hanley, J.E. Blalock, and R.B. Marchase. 1999. Calcium influx factor is synthesized by yeast and mammalian cells depleted of organellar calcium stores. *Proc. Natl. Acad. Sci. USA*. 96:121–126.

Fasolato, C., M. Hoth, and R. Penner. 1993. A GTP-dependent step in the activation mechanism of capacitative calcium influx. *J. Biol. Chem.* 268:20737–20740.

Feske, S., Y. Gwack, M. Prakriya, S. Srikanth, S.H. Puppel, B. Tanasa, P.G. Hogan, R.S. Lewis, M. Daly, and A. Rao. 2006. A mutation in Orai1 causes immune deficiency by abrogating CRAC channel function. *Nature*. 441:179–185.

Hofer, A.M., C. Fasolato, and T. Pozzan. 1998. Capacitative Ca2+ entry is closely linked to the filling state of internal Ca2+ stores: a study using simultaneous measurements of ICRAC and intraluminal. *J. Cell Biol.* 140:325–334.

Hoth, M., and R. Penner. 1992. Depletion of intracellular calcium stores activates a calcium current in mast cells. *Nature*. 355:353–356.

Irvine, R.F. 1990. 'Quantal' Ca2+ release and the control of Ca2+ entry by inositol phosphates–a possible mechanism. *FEBS Lett.* 263:5–9.

Ishiai, M., M. Kurosaki, R. Pappu, K. Okawa, I. Ronko, C. Fu, M. Shibata, A. Iwamatsu, A.C. Chan, and T. Kurosaki. 1999. BLNK required for coupling Syk to PLC gamma 2 and Rac1-JNK in B cells. *Immunity*. 10:117–125.

Jaconi, M.E., D.P. Lew, A. Monod, and K.H. Krause. 1993. The regulation of store-dependent Ca2+ influx in HL-60 granulocytes involves GTP-sensitive elements. *J. Biol. Chem.* 268:26075–26078.

Kiselyov, K., D.M. Shin, N. Shcheynikov, T. Kurosaki, and S. Muallem. 2001. Regulation of Ca2+-release-activated Ca2+ current (Icrac) by ryanodine receptors in inositol 1,4,5-trisphosphate-receptor-deficient DT40 cells. *Biochem. J.* 360:17–22.

Kurosaki, T. 2000. Functional dissection of BCR signaling pathways. *Curr. Opin. Immunol.* 12:276–281.

Lee, K.M., K. Toscas, and M.L. Villereal. 1993. Inhibition of bradykinin- and thapsigargin-induced Ca2+ entry by tyrosine kinase inhibitors. *J. Biol. Chem.* 268:9945–9948.

Lewis, R.S. 1999. Store-operated calcium channels. *Adv. Second Messenger Phosphoprotein Res.* 33:279–307.

Lewis, R.S., and M.D. Cahalan. 1989. Mitogen-induced oscillations of cytosolic Ca2+ and transmembrane Ca2+ current in human leukemic T cells. *Cell Regul.* 1:99–112.

Liou, J., M.L. Kim, W.D. Heo, J.T. Jones, J.W. Myers, J.E. Ferrell Jr., and T. Meyer. 2005. STIM is a Ca2+ sensor essential for Ca2+-store-depletion-triggered Ca2+ influx. *Curr. Biol.* 15:1235–1241.

Liu, K.Q., S.C. Bunnell, C.B. Gurniak, and L.J. Berg. 1998. T cell receptor-initiated calcium release is uncoupled from capacitative calcium entry in Itk-deficient T cells. *J. Exp. Med.* 187:1721–1727.

Luckhoff, A., and D.E. Clapham. 1992. Inositol 1,3,4,5-tetrakisphosphate activates an endothelial Ca(2+)- permeable channel. *Nature*. 355:356–358.

Luik, R.M., M.M. Wu, J. Buchanan, and R.S. Lewis. 2006. The elementary unit of store-operated Ca2+ entry: local activation of CRAC channels by STIM1 at ER-plasma membrane junctions. *J. Cell Biol.* 174:815–825.

Ma, H.T., K. Venkatachalam, H.S. Li, C. Montell, T. Kurosaki, R.L. Patterson, and D.L. Gill. 2001. Assessment of the role of the inositol 1,4,5-trisphosphate receptor in the activation of transient receptor potential channels and store-operated Ca2+ entry channels. *J. Biol. Chem.* 276:18888–18896.

McDonald, T.V., B.A. Premack, and P. Gardner. 1993. Flash photolysis of caged inositol 1,4,5-trisphosphate activates plasma membrane calcium current in human T cells. *J. Biol. Chem.* 268:3889–3896.

Mizuguchi, J., Y. Yamanashi, K. Ehara, T. Tamura, H. Nariuchi, Y. Gyotoku, H. Fukazawa, Y. Uehara, and T. Yamamoto. 1992. Tyrosine protein kinase is involved in anti-IgM-mediated signaling in BAL17 B lymphoma cells. *J. Immunol.* 148:689–694.

Mori, Y., M. Wakamori, T. Miyakawa, M. Hermosura, Y. Hara, M. Nishida, K. Hirose, A. Mizushima, M. Kurosaki, E. Mori, et al. 2002. Transient receptor potential 1 regulates capacitative Ca(2+) entry and Ca(2+) release from endoplasmic reticulum in B lymphocytes. *J. Exp. Med.* 195:673–681.

Nagao, Y., M. Noji, Y. Asano, T. Hamano, and M. Nakanishi. 1996. Calcium signals in helper T cells after interaction with antigen- specific and antigen-nonspecific B cells. *Biol. Pharm. Bull.* 19:697–700.

Onoda, T., H. Iinuma, Y. Sasaki, M. Hamada, K. Isshiki, H. Naganawa, T. Takeuchi, K. Tatsuta, and K. Umezawa. 1989. Isolation of a novel tyrosine kinase inhibitor, lavendustin A, from *Streptomyces griseolavendus*. *J. Nat. Prod.* 52:1252–1257.

Parekh, A.B., and R. Penner. 1995. Depletion-activated calcium current is inhibited by protein kinase in RBL-2H3 cells. *Proc. Natl. Acad. Sci. USA.* 92:7907–7911.

Parekh, A.B., and R. Penner. 1997. Store depletion and calcium influx. *Physiol. Rev.* 77:901–930.

Patterson, R.L., D.B. van Rossum, and D.L. Gill. 1999. Store-operated Ca2+ entry: evidence for a secretion-like coupling model. *Cell.* 98:487–499.

Peinelt, C., M. Vig, D.L. Koomoa, A. Beck, M.J. Nadler, M. Koblan-Huberson, A. Lis, A. Fleig, R. Penner, and J.P. Kinet. 2006. Amplification of CRAC current by STIM1 and CRACM1 (Orai1). *Nat. Cell Biol.* 8:771–773.

Petersen, C.C., and M.J. Berridge. 1995. G-protein regulation of capacitative calcium entry may be mediated by protein kinases A and C in *Xenopus* oocytes. *Biochem. J.* 307:663–668.

Petersen, C.C., and M.J. Berridge. 1996. Capacitative calcium entry is co-localised with calcium release in *Xenopus* oocytes: evidence against a highly diffusible calcium influx factor. *Pflugers Arch.* 432:286–292.

Ping, P., J. Zhang, Y.T. Zheng, R.C. Li, B. Dawn, X.L. Tang, H. Takano, Z. Balafanova, and R. Bolli. 1999. Demonstration of selective protein kinase C-dependent activation of Src and Lck tyrosine kinases during ischemic preconditioning in conscious rabbits. *Circ. Res.* 85:542–550.

Prakriya, M., and R.S. Lewis. 2001. Potentiation and inhibition of Ca(2+) release-activated Ca(2+) channels by 2-aminoethyldiphenyl borate (2-APB) occurs independently of IP(3) receptors. 536:3–19.

Premack, B.A., T.V. McDonald, and P. Gardner. 1994. Activation of Ca2+ current in Jurkat T cells following the depletion of Ca2+ stores by microsomal Ca(2+)-ATPase inhibitors. *J. Immunol.* 152:5226–5240.

Randriamampita, C., and R.Y. Tsien. 1993. Emptying of intracellular Ca2+ stores releases a novel small messenger that stimulates Ca2+ influx. *Nature.* 364:809–814.

Rawlings, D.J. 1999. Bruton's tyrosine kinase controls a sustained calcium signal essential for B lineage development and function. *Clin. Immunol.* 91:243–253.

Roos, J., P.J. DiGregorio, A.V. Yeromin, K. Ohlsen, M. Lioudyno, S. Zhang, O. Safrina, J.A. Kozak, S.L. Wagner, M.D. Cahalan, G. Velicelebi, and K.A. Stauderman. 2005. STIM1, an essential and conserved component of store-operated Ca2+ channel function. *J. Cell Biol.* 169:435–445.

Rosado, J.A., D. Graves, and S.O. Sage. 2000. Tyrosine kinases activate store-mediated Ca2+ entry in human platelets through the reorganization of the actin cytoskeleton. *Biochem. J.* 351:429–437.

Rosado, J.A., P.C. Redondo, S.O. Sage, J.A. Pariente, and G.M. Salido. 2005. Store-operated Ca2+ entry: vesicle fusion or reversible trafficking and de novo conformational coupling? *J. Cell. Physiol.* 205:262–269.

Sargeant, P., R.W. Farndale, and S.O. Sage. 1993a. ADP- and thapsigargin-evoked Ca2+ entry and protein-tyrosine phosphorylation are inhibited by the tyrosine kinase inhibitors genistein and methyl-2,5-dihydroxycinnamate in fura-2-loaded human platelets. *J. Biol. Chem.* 268:18151–18156.

Sargeant, P., R.W. Farndale, and S.O. Sage. 1993b. The tyrosine kinase inhibitors methyl 2,5-dihydroxycinnamate and genistein reduce thrombin-evoked tyrosine phosphorylation and Ca2+ entry in human platelets. *FEBS Lett.* 315:242–246.

Schieven, G.L., J.M. Kirihara, D.L. Burg, R.L. Geahlen, and J.A. Ledbetter. 1993. p72syk tyrosine kinase is activated by oxidizing conditions that induce lymphocyte tyrosine phosphorylation and Ca2+ signals. *J. Biol. Chem.* 268:16688–16692.

Scott, C.C., W. Furuya, W.S. Trimble, and S. Grinstein. 2003. Activation of store-operated calcium channels: assessment of the role of snare-mediated vesicular transport. *J. Biol. Chem.* 278:30534–30539.

Takata, M., and T. Kurosaki. 1996. A role for Bruton's tyrosine kinase in B cell antigen receptor-mediated activation of phospholipase C-γ 2. *J. Exp. Med.* 184:31–40.

Takata, M., H. Sabe, A. Hata, T. Inazu, Y. Homma, T. Nukada, H. Yamamura, and T. Kurosaki. 1994. Tyrosine kinases Lyn and Syk regulate B cell receptor-coupled Ca2+ mobilization through distinct pathways. *EMBO J.* 13:1341–1349.

Takeshima, H., T. Ikemoto, M. Nishi, N. Nishiyama, M. Shimuta, Y. Sugitani, J. Kuno, I. Saito, H. Saito, M. Endo, M. Iino, and T. Noda. 1996. Generation and characterization of mutant mice lacking ryanodine receptor type 3. *J. Biol. Chem.* 271:19649–19652.

Vazquez, G., B.J. Wedel, G.S. Bird, S.K. Joseph, and J.W. Putney. 2002. An inositol 1,4,5-trisphosphate receptor-dependent cation entry pathway in DT40 B lymphocytes. *EMBO J.* 21:4531–4538.

Vig, M., A. Beck, J.M. Billingsley, A. Lis, S. Parvez, C. Peinelt, D.L. Koomoa, J. Soboloff, D.L. Gill, A. Fleig, J.P. Kinet, and R. Penner. 2006a. CRACM1 multimers form the ion-selective pore of the CRAC channel. *Curr. Biol.* 16:2073–2079.

Vig, M., C. Peinelt, A. Beck, D.L. Koomoa, D. Rabah, M. Koblan-Huberson, S. Kraft, H. Turner, A. Fleig, R. Penner, and J.P. Kinet. 2006b. CRACM1 is a plasma membrane protein essential for store-operated Ca2+ entry. *Science.* 312:1220–1223.

Whisler, R.L., B.Q. Liu, Y.G. Newhouse, J.D. Walters, M.B. Breckenridge, and I.S. Grants. 1991. Signal transduction in human B cells during aging: alterations in stimulus-induced phosphorylations of tyrosine and serine/threonine substrates and in cytosolic calcium responsiveness. *Lymphokine Cytokine Res.* 10:463–473.

Wienands, J. 2000. Signal transduction elements of the B cell antigen receptor and their role in immunodeficiencies. *Immunobiology.* 202:120–133.

Wollscheid, B., J. Wienands, and M. Reth. 1999. The adaptor protein SLP-65/BLNK controls the calcium response in activated B cells. *Curr. Top. Microbiol. Immunol.* 246:283–288 (discussion 288–289).

Wu, M.M., J. Buchanan, R.M. Luik, and R.S. Lewis. 2006. Ca2+ store depletion causes STIM1 to accumulate in ER regions closely associated with the plasma membrane. *J. Cell Biol.* 174:803–813.

Yao, Y., A.V. Ferrer-Montiel, M. Montal, and R.Y. Tsien. 1999. Activation of store-operated Ca2+ current in *Xenopus* oocytes requires SNAP-25 but not a diffusible messenger. *Cell.* 98:475–485.

Yeromin, A.V., S.L. Zhang, W. Jiang, Y. Yu, O. Safrina, and M.D. Cahalan. 2006. Molecular identification of the CRAC channel by altered ion selectivity in a mutant of Orai. *Nature.* 443:226–229.

Zhang, S.L., Y. Yu, J. Roos, J.A. Kozak, T.J. Deerinck, M.H. Ellisman, K.A. Stauderman, and M.D. Cahalan. 2005. STIM1 is a Ca2+ sensor that activates CRAC channels and migrates from the Ca2+ store to the plasma membrane. *Nature.* 437:902–905.

Zhao, Q., and A. Weiss. 1996. Enhancement of lymphocyte responsiveness by a gain-of-function mutation of ZAP-70. *Mol. Cell. Biol.* 16:6765–6774.

Zweifach, A., and R.S. Lewis. 1993. Mitogen-regulated Ca2+ current of T lymphocytes is activated by depletion of intracellular Ca2+ stores. *Proc. Natl. Acad. Sci. USA.* 90:6295–6299.